Molecular Biology of the Cell
Vol. 19, 4421–4433, October 2008

DNA Topoisomerase II Is a Determinant of the Tensile Properties of Yeast Centromeric Chromatin and the Tension Checkpoint

Tariq H. Warsi, Michelle S. Navarro, and Jeff Bachant

Department of Cell Biology and Neuroscience, University of California, Riverside, Riverside, CA 92521

Submitted June 2, 2008; Revised July 29, 2008; Accepted August 6, 2008
Monitoring Editor: Kerry S. Bloom

Centromeric (*CEN*) chromatin is placed under mechanical tension and stretches as kinetochores biorient on the mitotic spindle. This deformation could conceivably provide a readout of biorientation to error correction mechanisms that monitor kinetochore–spindle interactions, but whether *CEN* chromatin acts in a tensiometer capacity is unresolved. Here, we report observations linking yeast Topoisomerase II (Top2) to both *CEN* mechanics and assessment of interkinetochore tension. First, in *top2-4* and sumoylation-resistant *top2-SNM* mutants *CEN* chromatin stretches extensively during biorientation, resulting in increased sister kinetochore separation and preanaphase spindle extension. Our data indicate increased *CEN* stretching corresponds with alterations to *CEN* topology induced in response to tension. Second, Top2 potentiates aspects of the tension checkpoint. Mutations affecting the Mtw1 kinetochore protein activate Ipl1 kinase to detach kinetochores and induce spindle checkpoint arrest. In *mtw1top2-4* and *mtw1top2-SNM* mutants, however, kinetochores are resistant to detachment and checkpoint arrest is attenuated. For *top2-SNM* cells, *CEN* stretching and checkpoint attenuation occur even in the absence of catenation linking sister chromatids. In sum, Top2 seems to play a novel role in *CEN* compaction that is distinct from decatenation. Perturbations to this function may allow weakened kinetochores to stretch *CEN*s in a manner that mimics tension or evades Ipl1 surveillance.

INTRODUCTION

Accurate chromosome segregation requires that sister kinetochores connect to microtubules from opposing poles of the mitotic spindle, a process known as biorientation. Misaligned kinetochore attachments can also occur, and they must be resolved to prevent lethal chromosome segregation errors or the formation of aneuploid cells. Syntelic attachments arise when sister kinetochores connect to microtubules from the same spindle pole; merotelic attachments result if a single kinetochore attaches to both poles. The Aurora-B kinases, complexed with conserved INCENP/Sli15 and Survivin/Bir1 subunits of the chromosomal passenger complex, are key regulators of the error correction machinery that resolves such inappropriate attachments (reviewed in Ruchaud *et al*., 2007). Aurora-B (Ipl1 in budding yeast) facilitates error correction through two mechanisms. First, these kinases destabilize defective kinetochore–microtubule interactions by phosphorylating kinetochore-associated proteins. Second, Ipl1/Aurora-B plays a role in activating the spindle assembly checkpoint (SAC), both in response to syntelic attachments as well as mutations that affect the kinetochore or sister chromatid cohesion. Checkpoint activation may occur indirectly because Ipl1/Aurora-B creates unoccupied kinetochores (Pinsky *et al*., 2006) or directly through phosphorylation of SAC regulators (King *et al*., 2007).

The manner in which Ipl1/Aurora-B distinguishes such a wide range of spindle lesions is not well understood. With the exception of merotelic interactions (Cimini, 2007), those attachments that are targeted for error correction generally tend to be characterized by a reduction in the mechanical tension generated by pulling bioriented kinetochores toward opposite spindle poles. Ipl1/Aurora-B has thus been suggested to control a tension checkpoint, implying a mechanism to monitor tension (Biggins and Murray, 2001). But whether tension is sensed directly, or transduced into an alteration of the kinetochore-microtubule interface that allows kinetochores to become resistant to Ipl1/Aurora-B, is a matter of debate (Pinsky and Biggins, 2005; Sandall *et al*., 2006). As one facet of this, it has long been recognized that elastic deformation of chromatin underlying and/or adjacent to the kinetochore (collectively denoted here as *CEN* chromatin) could provide a mechanical readout of biorientation (McIntosh, 1991; Shelby *et al*., 1996). In yeast, for example, kinetochores are drawn apart to half the length of the preanaphase spindle by bipolar force, accompanied by a localized dissolution of *CEN* cohesion and partial unraveling of separated *CEN* fibers (He *et al*., 2000; Pearson *et al*., 2001; Eckert *et al*., 2007; Ocampo-Hafalla *et al*., 2007). Recent evidence suggests these separated regions fold back to form a cruciform structure that behaves as an integrated tensile unit, stretching and relaxing as kinetochores oscillate on the spindle (Yeh *et al*., 2008). Ipl1/Aurora-B could be coupled to *CEN* deformation in a variety of ways. In one model, stretching of *CEN* fibers and/or components of the kinetochore under tension has been proposed to separate Ipl1/Aurora-B within the inner *CEN* from the kinetochore substrates in-

This article was published online ahead of print in *MBC in Press* (http://www.molbiolcell.org/cgi/doi/10.1091/mbc.E08–05–0547) on August 13, 2008.

Address correspondence to: Jeff Bachant (jeffbach@citrus.ucr.edu).

Abbreviations used: APC, anaphase promoting complex; *CEN*, centromere; GFP, green fluorescent protein; NZ, nocodazole; SAC, spindle assembly checkpoint; Topo II, DNA topoisomerase II; WT, wild type.

volved in detachment (Tanaka *et al*., 2002; Cimini, 2007). Overall, these considerations suggest the mechanical resistance of *CEN* chromatin to deformation could be an important parameter influencing the activity of error correction mechanisms.

Several observations indicate DNA Topoisomerase II (Topo II or Top2 in yeast) may be one factor that that is connected to Ipl1/Aurora-B in the tension checkpoint. First, in vertebrates Topo II accumulates and exhibits robust activity within mitotic *CEN* chromatin (reviewed in Porter and Farr, 2004). Sumoylation of Topo II (or possibly other substrates) plays an as yet undefined role in controlling Topo II localization to *CEN*s (Azuma *et al*., 2005; Diaz-Martinez *et al*., 2006; Dawlaty *et al*., 2008). Treatments that block this modification also perturb sister chromatid separation during anaphase, suggesting Topo II *CEN* targeting helps resolve a final population of topological intertwinings (catenates) so sister *CEN*s can disjoin efficiently. Second, in both yeast and vertebrates, Topo II inhibition can restore chromatid attachment to the spindle and silence the tension checkpoint in cohesin mutants, an effect that may be attributable to unresolved catenates substituting for cohesin in generating tension (Dewar *et al*., 2004; Vagnarelli *et al*., 2004; Toyoda and Yanagida, 2006). Third, perturbations to Topo II can in some cases activate Ipl1/Aurora-B–dependent preanaphase arrest (Andrews *et al*., 2006; Diaz-Martinez *et al*., 2006). This has suggested Ipl1/Aurora-B may be involved in monitoring some aspect of Topo II function, but the basis for this surveillance has remained unclear.

In this report, we find that budding yeast Top2 also plays an unanticipated role in helping Ipl1 enforce the tension checkpoint. Specifically, mutations in the Mtw1 kinetochore protein lead to weakened microtubule attachments that are disconnected by Ipl1. In temperature-sensitive *top2-4* mutants and *top2-SNM* mutants that prevent Top2 SUMO modification, however, these defective attachments are stabilized. In the case of *top2-SNM* mutants it is possible to show that stabilization of attachment does not occur through catenates restoring tension to *mtw1* kinetochores. Rather, the tension checkpoint defects associated with *top2* mutants correspond more closely with a requirement for Top2 in preventing excessive *CEN* stretching as sister kinetochores are pulled toward opposite spindle poles. These results suggest the ability of *CEN* chromatin to resist spindle traction may indeed be connected to tension assessment mechanisms. In this view, sumoylation promotes an aspect of Top2 function that maintains *CEN* compaction against poleward force. Perturbations to this function could allow weakened kinetochores to stretch *CEN* chromatin into a configuration that confers resistance to Ipl1 detachment activity.

MATERIALS AND METHODS

Yeast Strain Construction and Culture Conditions

All strains were derived from W303-related CRY1 (*MATa his3-11,15 leu2-3112 trp1-1 ura3-1 ade2-1 can1-100*) by using standard genetic techniques. *CEN4-GFP* comprises 256 copies of the Lac operator targeted 705 base pairs to the right side of *CEN4* CDEIII (Bachant *et al*., 2002). *Saccharomyces cerevisiae* were cultured in yeast extract/peptone/dextrose (YPD) or synthetic complete media. Cultures for microscopy were supplemented with 50 μg/ml adenine. For G_1 synchronization, overnight cultures were diluted into fresh media supplemented with 10 μg/ml α-factor (Bio-Synthesis, Lewisville, TX) for 2–3 h; *bar1* strains were treated with 1 μg/ml. Cells were washed in H_2O and released in fresh media at an appropriate temperature. Efficient release at 37°C required addition of 0.1 mg/ml Pronase (P-6911; Sigma-Aldrich, St. Louis, MO). For α-factor add-back, cells were released into YPD, pH 3.9, and α-factor was restored (20 μg/ml) when ~80% of the cells exhibited a small budded morphology. Nocodazole (Sigma-Aldrich) was dissolved in dimethyl sulfoxide at 10 mg/ml and used at a final concentration of 15 μg/ml in YPD.

Strains for in situ *CEN* excision were constructed as follows. A 1408-base pair SpeI-XhoI fragment from YCp50 containing *CEN4* was cloned into pLITMUS29 (pJBN137). A 450-base pair AvrII fragment containing *CEN4* CDE I-II-III elements on pJBN137 was replaced with a 3576-base pair *loxP(CEN1:kanMX4)loxP* cassette to form pJBN150. The elements on this cassette include two *lox*P sites from pSE934, a *CEN1* sequence originating from a 1769-base pair HindIII fragment from YRp14/ARS1/CEN (Hieter *et al*., 1985), chromosome I (base pairs 150402–152170), and a 1561-base pair NotI fragment from pFA6a/*kanMX4* containing *kanMX4* (Wach *et al*., 1994). To replace *CEN4* with *loxP(CEN1:kanMX4)loxP*, a CRY1 *TRP1-GFP* strain was transformed with a 4522-base pair fragment derived from pJBN150 by SpeI-XhoI digestion. Transformants were selected for G418 resistance, and *CEN4* replacement was verified by the appearance of a novel 4534-base pair XhoI fragment on Southern blots by using a 1408-base pair *CEN4* SpeI-XhoI fragment isolated from pJBN137 to prepare radiolabeled probes. Standard genetic crosses were used to transfer *loxCENlox* to other strains. To induce *CEN* excision, *loxP(CEN1:kanMX4)loxP* strains were transformed with pBS49 (p*GAL-Cre CEN/ARS/URA3*; Sauer, 1987) and processed into galactose media.

Microscopy

For Pds1-Myc immunofluorescence, ~5×10^6 cells were fixed in 3.7% formaldehyde for 2–4 h and spheroplasted (15 min; 37°C) in 0.5 ml of 1.2 M sorbitol, 100 mM KPO_4, pH 7.5, containing 1 μl of β-mercaptoethanol (β-ME) and 5 μl of 5 mg/ml Zymolyase 100-T (MP Biomedicals, Irvine, CA). Spheroplasts were resuspended in 0.5 ml of phosphate-buffered saline (PBS), 0.1% Triton X-100 (PBS: 150 mM NaCl, 50 mM KPO_4, pH 7.5); this permeabilization step was essential for Pds1-Myc staining. Staining was performed by sequential incubation in 50 μl of a 1:100 dilution of 9E10 (Covance Research Products, Princeton, NJ) (diluted in PBS; 1–2 h; room temperature) and 50 μl of a 1:250 dilution of fluorescein isothiocyanate (FITC)-conjugated α-mouse antibodies (Jackson ImmunoResearch Laboratories, West Grove, PA). Stained specimens were washed into PBS and spotted onto 0.1% poly-lysine–coated slides. For α-tubulin immunofluorescence, cells were fixed 4–15 h, permeabilized in 70% ethanol, spheroplasted 1 h, and stained using a 1:50 dilution of YOL1/34 (Accurate Chemical & Scientific, Westbury, NY) and a 1:100 dilution of FITC-conjugated α-rat antibodies (Sigma-Aldrich).

For budding analyses, *SPC42-GFP* measurements, and 4,6-diamidino-2-phenylindole (DAPI) staining, cells were fixed in 3.7% formaldehyde for 3 min and washed into PBS. DAPI staining (1 μg/ml) was performed in mounting medium (VECTASHIELD; Vector Laboratories, Burlingame, CA). For *TRP1-GFP* (GFP, green fluorescent protein) separation/segregation kinetics, cells were fixed in 0.05% NaN_3 and 2.5 mM EDTA, washed into STOP solution (0.9% NaCl, 1 mM NaN_3, and 10 mM EDTA), and stored at 4°C. Visualization of *CEN4-GFP* and Ask1-GFP was performed using live cell mounts on a thermal stage (Tokai Hit, Shizuoka-ken, Japan), a 100× Plan Apo 1.4 numerical aperture objective and a number 4 neutral density filter. Spindle length and Ask1-GFP measurements were performed using MetaMorph software (Molecular Devices, Sunnyvale, CA). Live cell imaging was performed as described previously (Bachant *et al*., 2005). The statistical significance of differences between strains in the distribution of *CEN* stretching lengths, interkinetochore distance, and preanaphase spindle extension were evaluated using Student's *t* test.

Chromosome Loss Assays

Cells from single colonies cultured to maintain CFIII (Ura^- or Ade^-) were resuspended in H_2O, inoculated into YPD at low density, and grown to saturation. Cell density was determined at the beginning and end of the culture by using a hemacytometer, and the number of cell divisions (n) was calculated as $[\log_2(\text{final cell number}) - \log_2(\text{initial cell number})]$. CFIII loss was monitored either by plating a defined number of cells onto 5′-fluoroorotic acid media or by plating ~750 cells onto YPD and dividing the number of solid red colonies by total colony number. Using these values, the rate of CFIII loss per division (p) was determined using the equation $p = 1 - e^{(1/n)\ln(Rn/R0)}$, where R0 and Rn are the fraction of cells containing CFIII after 0 and n generations under nonselective conditions, respectively (Murakami *et al*., 1995). The significance of loss rate or frequency differences between strains was assessed using Student's *t* test.

Minichromosome Catenation and CEN Topoisomer Analysis

For analysis of minichromosome catenation, DNA was prepared from 10 ml of OD_{600} 0.8 cultures synchronized as appropriate for the experiment. Cells were spheroplasted (1 h; 37°C) in 0.6 ml of 0.9 M sorbitol, 100 mM EDTA, a 1:500 dilution of β-ME, and 0.3 mg/ml Zymolyase 20T (MP Biomedicals). Spheroplasts were resuspended in 0.6 ml of TE (20 mM Tris, pH 8.0, and 2 mM EDTA) and lysed (65°C; 30 min) by adding 240 μl of 250 mM EDTA, 0.5 M Tris base, and 2.5% SDS. Then, 400 μl of 5 M KOAC was added to the solution, which was incubated on ice for 1 h and clarified at 13.5K rpm (15 min; 4°C). Nucleic acids were precipitated using isopropanol, resuspended in 500 μl of TE containing 50 μg/ml RNase, and incubated for 1 h at 37°C. After a second precipitation (adding 20 microliters SM NaCl), DNA was dissolved

in 40 μl of TE. Then, 7 μl of the sample was loaded onto wide (2.3-cm) well format 20- by 20-cm 0.6% agarose gels containing ethidium bromide (0.5 μg/ml) and electrophoresed in 1× TAE overnight at 50-V constant voltage. Southern transfer was carried out under alkaline conditions onto Hybond-XL (GE Healthcare, Little Chalfont, Buckinghamshire, United Kingdom) membranes. Radiolabeled probes to detect both p3847 and pRS416 were synthesized using a 1549-base pair ScaI/PvuII fragment from pRS416. Hybridization was performed in RapidHyb (GE Healthcare) according to manufacturer's instructions. For analysis of *CEN* loop-out topoisomers, DNA was prepared from 50 ml of saturated cultures that were refed and processed as described in the legend for Figure 5. Genomic DNA was prepared as described for catenation samples, scaling up as appropriate for the larger cultures. The final DNA prep was resuspended in 200 μl of TE, and 50 μg of each sample was separated on 25- × 20 cm 1% agaraose gels in TAE containing an appropriate concentration of chloroquine in both the gel and running buffer. Electrophoresis and Southern transfer was carried out as described for catenation samples, but electrophoresis time was extended to 24 h, and ethidium bromide was omitted from both the gel and running buffer. The use of wide (2.3 cm) wells and extended electrophoretic separation proved essential for resolution of linking number variants. *CEN* topoisomers were visualized with radiolabeled probes prepared from a 1087-base pair DNA fragment amplified from pFA6a-*kanMX4* (Wach *et al.*, 1994) by using primers JB.101 5′-CCGAACATAAAGCGGCCGCGGTAAGGAAAAGACTCACGTTTCGAGGC and JB.102 5′-ATCGATGAATTCGAGCTCGTTTTCGACACTGGATGGC.

To create the *CEN* topoisomers profiles shown in Figure 5 and Supplemental Figure 4, digitized images of Southern autoradiograms were analyzed using the plot profile features of NIH ImageJ software (http://rsb.info.nih.gov/ij/), ensuring all gray scale values were in the nonsaturated range. Y coordinate values were normalized such that the highest topoisomer band for each sample (not the nicked/relaxed circle form) was assigned a relative gray scale value of 1. This allowed the profile plots to be overlaid directly in a graphical representation.

Protein Analysis

Protein extracts for immunoblotting were prepared using mechanical lysis in 20% trichloroacetic acid as described previously (Bachant *et al.*, 2002).

RESULTS

Sister Chromatid Separation and Segregation in top2-SNM Mutants

Accumulating evidence suggests Topo II sumoylation promotes sister chromatid decatenation and chromosome segregation in vertebrate cells (Azuma *et al.*, 2003, 2005; Diaz-Martinez *et al.*, 2006; Dawlaty *et al.*, 2008), but whether this modification played an analogous role in yeast Top2 function was unclear. To evaluate functions associated with Top2 sumoylation, we therefore initially compared the catenation status of pRS416, a topologically closed circular minichromosome, in *top2-SNM* and *top2-4* mutants. The *top2-SNM* allele consists of mutations within the noncatalytic C-terminal domain that abolish SUMO modification (Bachant *et al.*, 2002; Takahashi *et al.*, 2006). *top2-4* is a well-characterized temperature-sensitive allele (DiNardo *et al.*, 1984; Holm *et al.*, 1985). Because the force of the spindle has been proposed to help resolve catenates (Holm, 1994), we isolated pRS416 from mitotic cells in the presence or absence of a spindle. Wild-type (WT), *top2-SNM*, and *top2-4* cells were arrested using nocodazole to depolymerize microtubules, whereas *cdc13-1*, *cdc13-1top2-4*, and *cdc13-1top2-SNM* cells were arrested in the presence of a spindle at a *cdc13-1* mitotic block. *cdc13-1* induces telomeric DNA damage and activates mitotic arrest through the DNA damage checkpoint (Garvik *et al.*, 1995). Consistent with previous studies (Koshland and Hartwell, 1987), we found pRS416 was completely decatenated under both arrest conditions in WT cells, whereas catenated dimers accumulated in *top2-4* strains. Similar to WT controls, only supercoiled and nicked forms of pRS416 were observed in *top2-SNM* mutants (Figure 1A).

Although minichromosomes are decatenated before anaphase, Top2 must act at the metaphase–anaphase transition to resolve catenates that persist on endogenous chromosomes. This decatenation activity is essential for sister chromatids to disjoin completely (Holm *et al.*, 1989). In particular, it has been shown that *CEN*s separate normally in *top2-4* cells, whereas telomeric regions fail to disjoin, suggesting catenates may roll down chromosome arms as sisters are pulled apart (Spell and Holm, 1994; Bhalla *et al.*, 2002). To determine whether Top2 SUMO modification facilitated sister separation, we examined chromatid disjunction at *CEN*-proximal (*TRP1-GFP*; 13kb from *CEN4*) and telomere-proximal (*TEL4-GFP*; 94kb from right end of chromosome 4) loci in *top2-4* and *top2-SNM* strains. As evaluated by degradation of the anaphase inhibitor Pds1, *top2-4* and *top2-SNM* cells entered anaphase with similar kinetics to WT controls, although a fraction of Pds1 was stabilized in the *top2-4* strain (Figure 1B). As anticipated, WT, *top2-4* and *top2-SNM* cells displayed similar kinetics of separation and segregation at the *CEN* proximal locus (Figure 1C), whereas *top2-4* mutants were largely blocked for separation at telomeres (Figure 1D). DAPI staining revealed the block to telomere disjunction was accompanied by extensive chromosome bridging (Supplemental Figure 1). In comparison, *top2-SNM* mutants also exhibited a slight delay in telomere separation (Figure 1D) and a transient accumulation of stretched anaphase chromosomes (Supplemental Figure 1). However, chromatids seemed to eventually disjoin completely and segregate to spindle poles. Consistent with this, *top2-SNM* cells did not exhibit an increased rate of chromosome missegregation (Supplemental Figure 2A). Furthermore, deletion of *RAD52*, required for repair of DNA double-strand breaks, did not affect *top2-SNM* survival (data not shown) or chromosome loss (Supplemental Figure 2A), arguing transient stretching does not cause chromosome breakage. Overall, these results indicate Top2 sumoylation is dispensable for decatenating small minichromosomes but makes a minor contribution to the timing of chromatid disjunction on endogenous chromosomes. *top2-SNM* mutants may therefore experience a subtle perturbation to chromosome decatenation. If so, this perturbation that does not obviously interfere with chromosome segregation accuracy.

CEN Tensioning in top2-SNM and top2-4 Mutants

Having evaluated whether Top2 sumoylation contributes to the overall program of anaphase chromosome separation and segregation, we next focused on possible roles for this modification in *CEN* chromatin dynamics (here, we use the term *CEN* chromatin to encompass both the *CEN* locus and adjacent peri*CEN* regions). We felt this might be informative because in vertebrates sumoylation seems to preferentially promote Topo II function at *CEN*s (Diaz-Martinez *et al.*, 2006; Dawlaty *et al.*, 2008). *CEN* dynamics during kinetochore biorientation have been characterized extensively in yeast, primarily using GFP tags integrated immediately adjacent to the kinetochore (Goshima and Yanagida, 2000; He *et al.*, 2000; Tanaka *et al.*, 2000; Pearson *et al.*, 2001). These studies have shown that sister *CEN*s are locally pulled apart as sister kinetochores attain bipolar attachment, accompanied by stretching of separated *CEN* chromatin. This initial distension, however, is quickly followed by a localized recompaction of the separated chromatid fibers.

As a first step in analyzing *CEN* dynamics, we examined *CEN* morphology in cycling *top2-SNM* mutants. Twenty-three percent of medium/large-budded *top2-SNM* cells exhibited a filamentous *CEN4-GFP* morphology distinct from the compact, spherical foci typically associated with bipolar attachment; a similar morphology was only observed in 7% of WT controls (Supplemental Figure 3, A and B). Direct measurement suggested *CEN4-GFP* was indeed drawn into

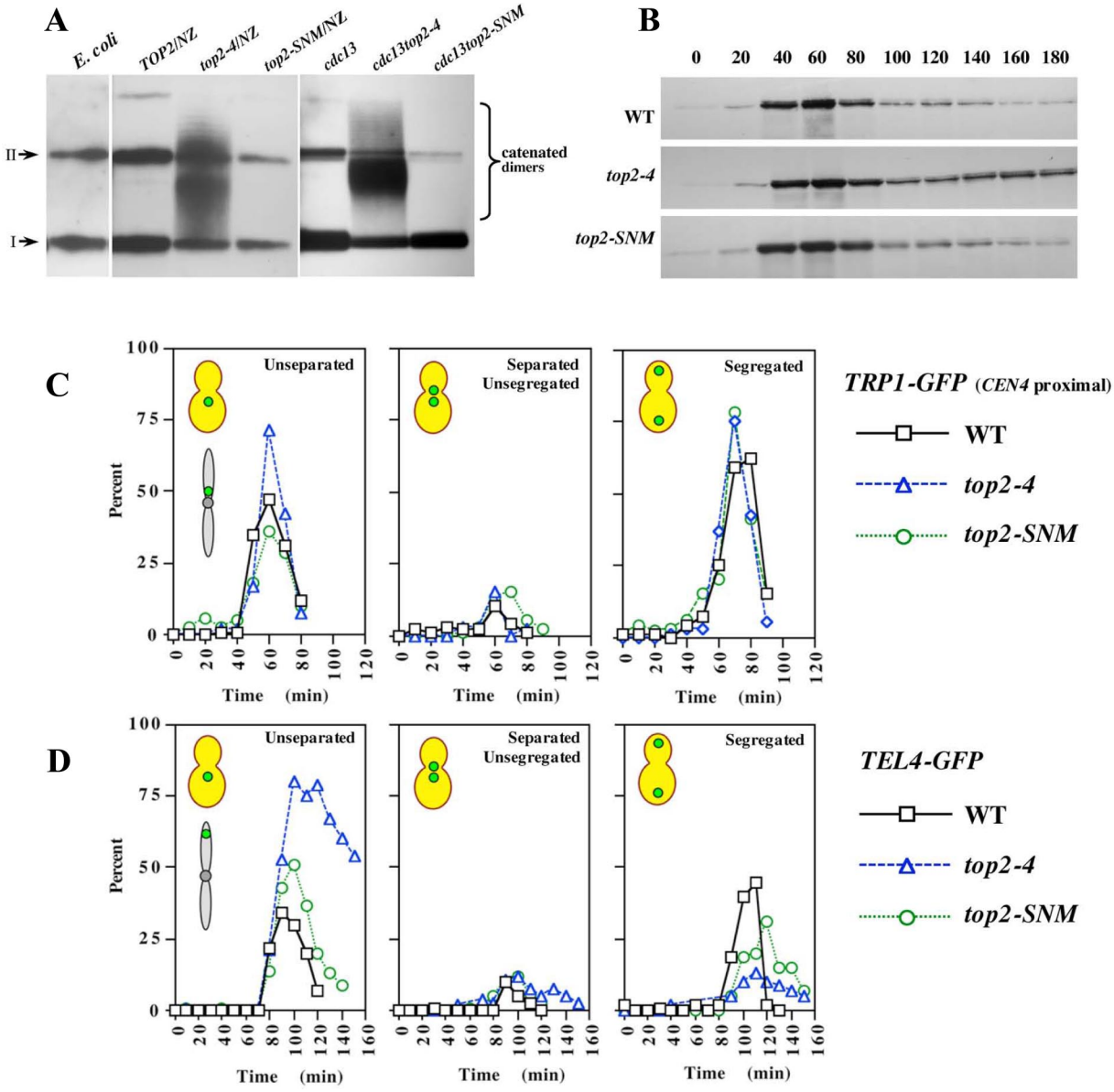

Figure 1. Chromosome decatenation and segregation in *top2-SNM* Mutants. (A) WT (*TOP2*; JBY772), *top2-4* (JBY775), *top2-SNM* (TWY179), *cdc13-1* (TWY181), *cdc13-1top2-4* (TWY185), and *cdc13top2-SNM* (TWY183) strains harboring pRS416 were released from α-factor at 35°C either in the presence (*CDC13* strains) or absence (*cdc13* strains) of nocodazole. After 3 h, pRS416 electrophoretic mobility was evaluated by Southern blotting. A bacterial plasmid preparation (*E. coli*) was included as a control. I and II denote supercoiled and nicked circular plasmid species. (B) WT (JBY649), *top2-4* (JBY1523) and *top2-SNM* (JBY1520) *PDS1-MYC* strains were arrested in G1 with α-factor, released at 35°C, and α-factor was restored after budding to rearrest cells in G1 after completion of mitosis. Pds1-myc was analyzed by immunoblotting. (C) WT (MNY37-8B), *top2-4* (MNY37-24A), and *top2-SNM* (MNY44-3D) *TRP1-GFP* strains were released from α-factor at 37°C and rearrested following completion of mitosis. The percentage of budded cells displaying unseparated *TRP1-GFP* foci (first graph), separated but unsegregated *TRP1-GFP* foci (second graph) and segregated *TRP1-GFP* foci (third graph) was determined at each time point. (D) WT (MNY46-3C), *top2-4* (MNY33-7C), and *top2-SNM* (MNY46-9C) *TEL4-GFP* strains were processed and analyzed as described in C.

a more extended configuration in *top2-SNM* cells (Supplemental Figure 3C). Importantly, our previous work indicated *top2* mutants remain largely proficient for chromatid cohesion at *CEN*-proximal chromosomal regions (Bachant *et al*., 2002). Thus, the extension of *CEN* chromatin in *top2* mutants is likely to reflect increased chromatid stretching rather than increased chromatid separation, and we therefore refer to this extension as a *CEN* stretching phenotype. To ensure we were not visualizing *CEN* stretching in early anaphase, we examined *CEN* morphology in metaphase-arrested *cdc13top2-SNM* and *cdc13top2-4* strains. Compared with *cdc13* controls, both *top2* mutants exhibited an approximately threefold increase in cells exhibiting *CEN4-GFP* stretching, corresponding with a reduction in cells with two discrete *CEN4-GFP* foci (Figure 2, A and B). This was not a consequence of *cdc13-1* DNA damage, as a similar type of stretching occurred in *top2-SNM* mutants blocked in metaphase by inactivating the anaphase-promoting complex (APC; Figure 2A).

CEN dynamics were further characterized by imaging cells over a 20-min period (Supplemental Videos 1–4). In *cdc13TOP2* cells, bioriented *CEN* foci remained close to-

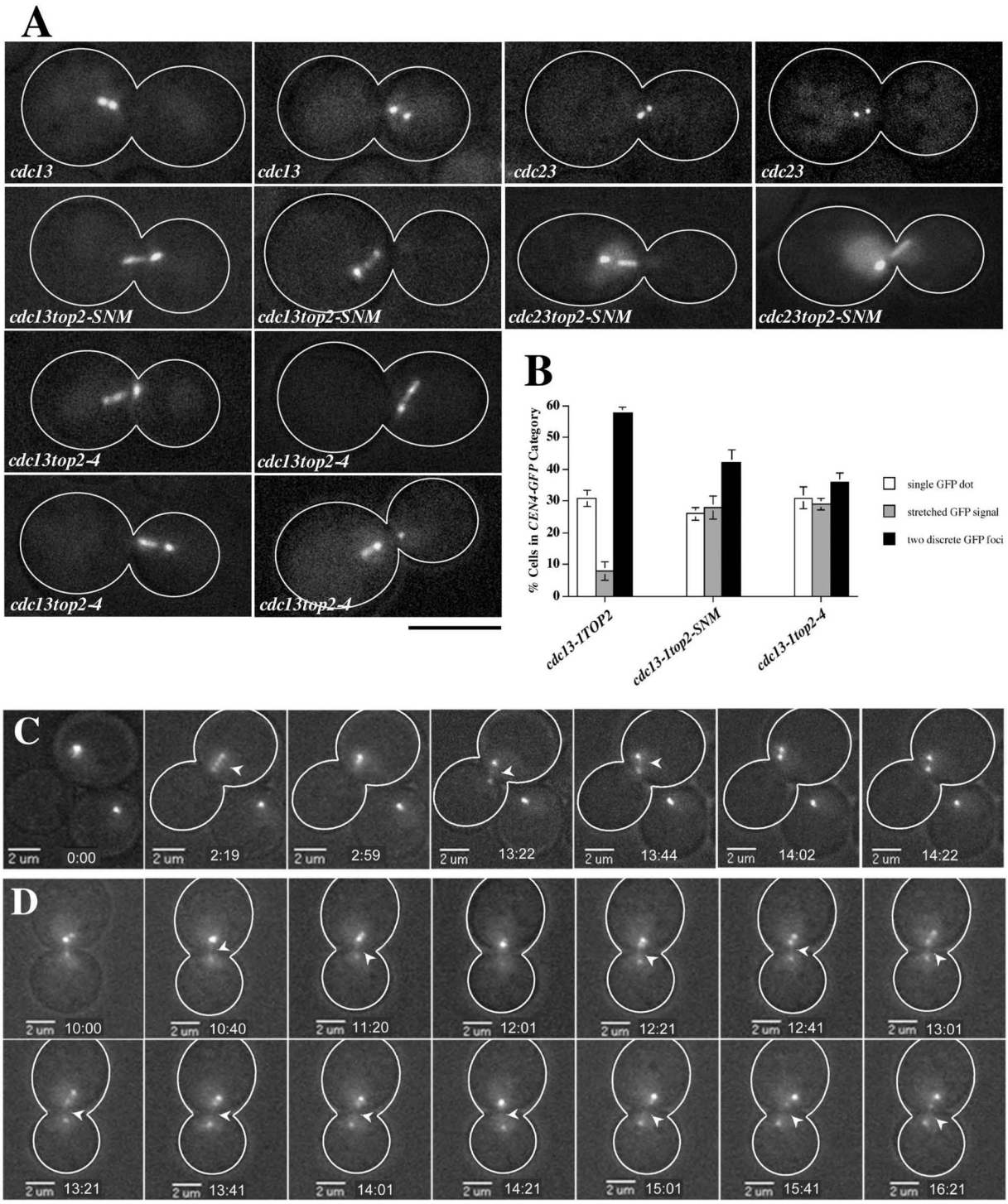

Figure 2. *CEN4-GFP* Stretching in *top2-4* and *top2-SNM* Mutants. (A) *cdc13-1* (JBY607), *cdc23-1* (JBY686), *cdc13-1top2-SNM* (JBY1100), *cdc23-1top2-SNM* (JBY1633), and *cdc13-1top2-4* (JBY845) *CEN4-GFP* strains were arrested at 32°C for 2.5 h before imaging. Micrographs illustrate bioriented *CEN4-GFP* foci in *cdc13* and *cdc23* cells and *CEN4-GFP* stretching in *top2* mutants. Bar, 5 μm. (B) *cdc13-1* (JBY607; 3 experiments), *cdc13-1top2-SNM* (JBY1100; 3 experiments), and *cdc13-1top2-4* (JBY845, JBY846; 2 experiments each) *CEN4-GFP* cells were processed for microscopy as in A and scored using the indicated categories. Graphs depict the average and SD for the combined experiments. (C) Selected frames showing a *cdc13TOP2* cell exhibiting *CEN4-GFP* stretching and separation into two compact foci. Numbers, elapsed time; arrows, *CEN4-GFP* stretching into a filamentous configuration. (D) Sequential frames illustrating *cdc13top2-SNM CEN4-GFP* stretching.

gether, and stretching events were of short duration. For example, Figure 2C depicts stretched *CEN4-GFP* chromatin that coalesces into a single GFP focus after 40 s. A second stretching event occurs that quickly resolves into two compact, spherical foci. In *cdc13top2-SNM* cells it proved difficult to visualize stretched *CEN* fibers for extended periods without photobleaching. However, based on successfully imaging five cells for a complete 20-min sequence, stretching of

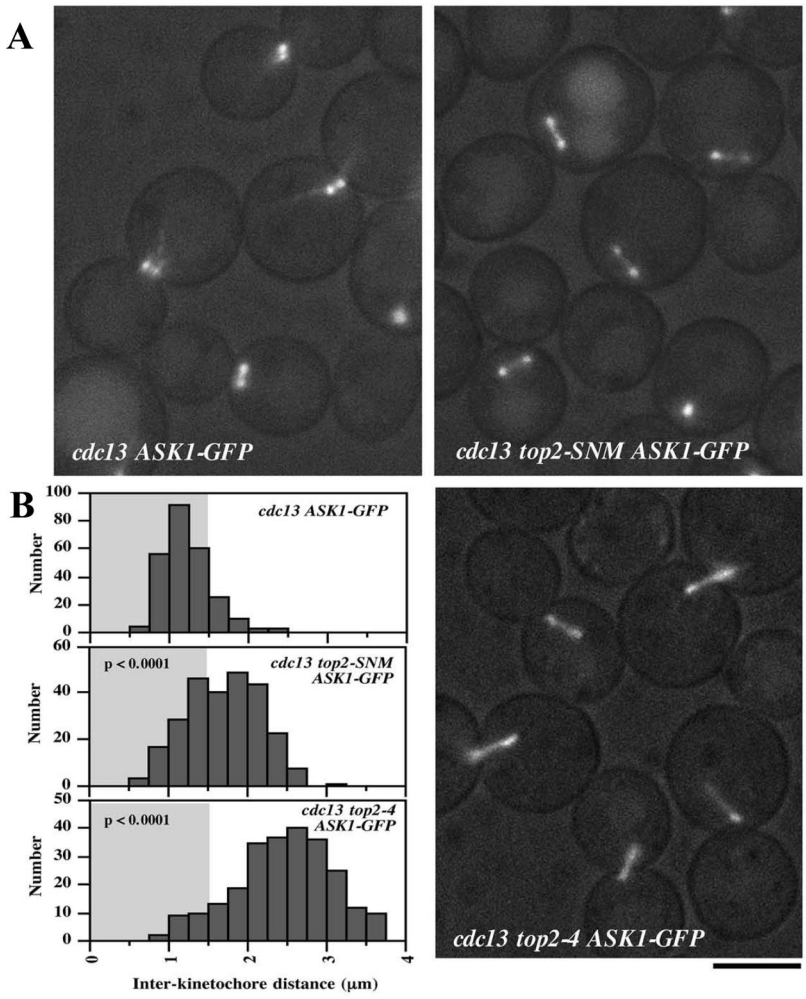

Figure 3. Interkinetochore distance in *top2-SNM* and *top2-4* Mutants. (A) *cdc13-1* (JBY1483), *cdc13-1top2-SNM* (JBY1485) and *cdc13-1top2-4* (JBY1694) *ASK1-GFP* cells were arrested for 2.5 h at 35°C and visualized by fluorescence microscopy. Bar, 5 μm. (B) *cdc13-1*, *cdc13-1top2-SNM*, and *cdc13-1top2-4 ASK1-GFP* cells were arrested and visualized as in A. For each strain, the distance between Ask1-GFP foci was measured for ≥250 cells. Histograms show the distribution of these measurements. p values indicate the significance of the differences between the *cdc13-1top2-SNM* and *cdc13-1top2-4* distributions compared with the *cdc13-1* control.

CEN4-GFP arrays seemed more persistent in *top2-SNM* cells (≥6 min for the cell in Figure 2D), suggesting recompaction to form closely juxtaposed foci occurred less efficiently.

A notable feature of the above-mentioned analysis was that *CEN* chromatin displayed an extent of stretching during biorientation in *top2-SNM* mutants that was comparable to the catalytically inactive *top2-4* allele. This suggested to us that sumoylation might be promoting a functional role for Top2 in endowing *CEN* fibers with the tensile properties to resist spindle traction. We reasoned that if this were true we would expect to observe an increased distance between bioriented kinetochores in both *top2* mutants, a parameter frequently used to evaluate the magnitude of interkinetochore tension. To test this we visualized the distribution of bioriented kinetochore clusters in *cdc13top2-SNM* and *cdc13top2-4* cells using Ask1-GFP, a component of the Dam1 kinetochore complex (Li *et al*., 2002). This analysis revealed kinetochores were in fact pulled further apart in both *top2* strains with mean distances of Ask1-GFP separation of 1.24 ± 0.34, 1.69 ± 0.47, and 2.46 ± 0.62 μm, respectively, in *TOP2*, *top2-SNM* and *top2-4* strains (Figure 3). Consistent with the normal chromosome loss rate of *top2-SNM* cells (Supplemental Figure 2A), increased kinetochore separation was not accompanied by obvious perturbations to kinetochore alignment. However, chromosome loss was slightly (~2-fold) but significantly ($p = 0.0002$) increased in Δ*mad2top2-SNM* strains (Supplemental Figure 2B), indicating the SAC contributes to chromosome segregation fidelity in *top2-SNM* cells. This suggests there may be infrequent kinetochore alignment problems in the *top2-SNM* mutant.

As a second metric for tension, we compared preanaphase spindle lengths in *cdc13* (mean length, 1.69 ± 0.42 μm), *cdc13top2-SNM* (2.17 ± 0.76 μm), *cdc13top2-4* (2.83 ± 0.73 μm), and *cdc13ubc9-1* (2.08 ± 0.59 μm) strains by using α-tubulin immunofluorescence (Figure 4, A and B) and in *cdc13* (mean pole separation, 2.49 ± 0.50 μm), *cdc13top2-SNM* (3.20 ± 0.67 μm), *cdc23* (2.87 ± 0.70 μm), and *cdc23top2-SNM* (3.67 ± 0.91 μm) cells by visualizing GFP-labeled spindle poles (Figure 4, C and D). Both methods of measurement indicated a statistically significant increase in spindle length in *top2* mutants. *cdc13ubc9-1* mutants, defective for SUMO conjugation, displayed similar spindle extension to *cdc13top2-SNM* cells. To summarize the results in this section, we observed that *CEN* chromatin is more prone to stretch in *top2-4* and *top2-SNM* strains, corresponding with increased sister kinetochore separation during biorientation and an accompanying increase in the length of the preanaphase spindle.

CEN Superhelicity in top2 Mutants

Current evidence suggests at least three possible functions for Top2 within *CEN* chromatin. First, a primary function for Topo II at *CEN*s, at least in vertebrates, seems to be untangling sister *CEN*s as cells transition into anaphase (Downes

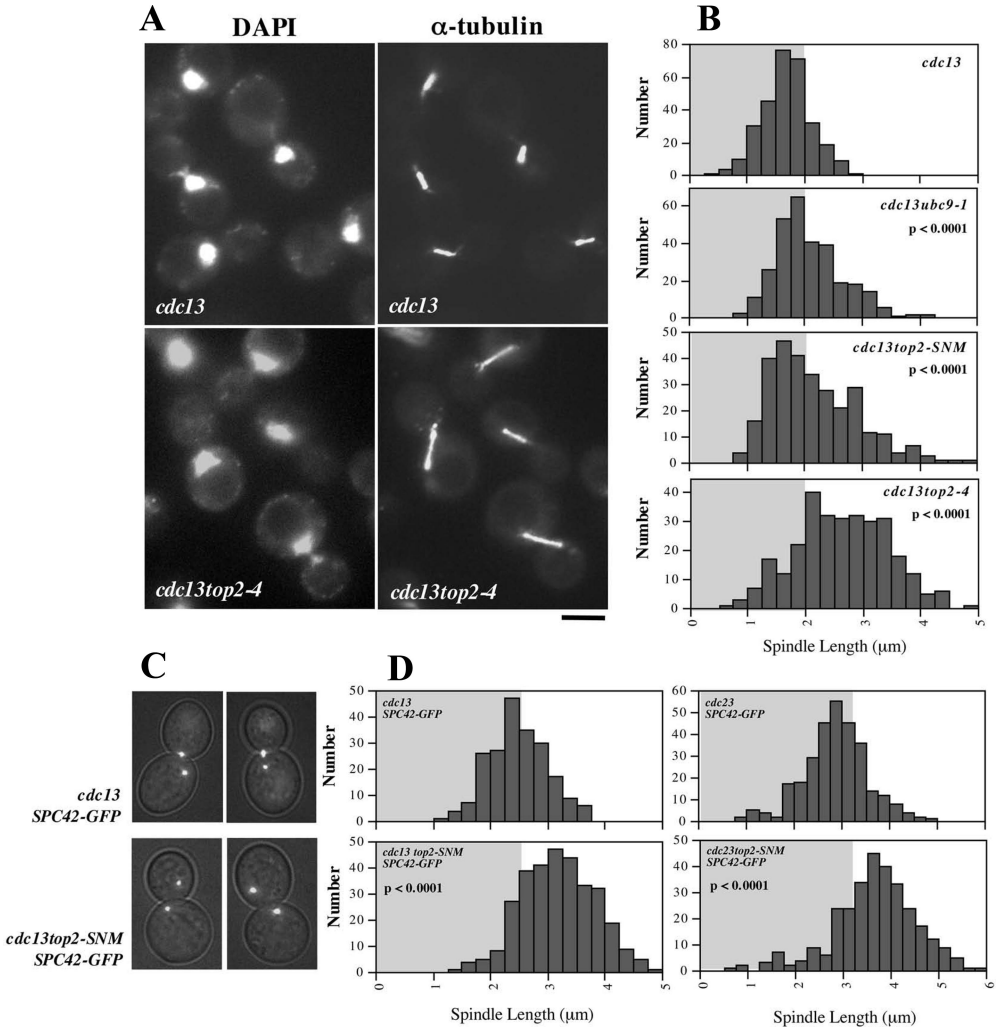

Figure 4. Preanaphase Spindle Length in *top2-4* and *top2-SNM* Mutants. (A) *cdc13-1* (JBY432) and *cdc13-1top2-4* (JBY626) strains were shifted to 35°C for 3 h and processed for α-tubulin immunofluorescence and DAPI staining. Bar; 5 μm. (B) Spindle length was measured in ≥300 *cdc13-1* (JBY607), *cdc13-1ubc9-1* (JBY1009), *cdc13top2-SNM* (JBY1100), and *cdc13-1top2-4* (JBY846) cells arrested as in A. Histograms show the distribution of spindle lengths. (C) *cdc13-1* (TWY001) and *cdc13-1top2-SNM* (TWY004) *SPC42-GFP* strains were arrested at 32°C for 3 h before imaging. (D) *cdc13-1*, *cdc13-1top2-SNM*, *cdc23-1* (JBY1289), and *cdc23-1top2-SNM* (JBY1601) *SPC42-GFP* strains were arrested as in C, and the distance between Spc42-GFP foci was evaluated in ≥300 cells. In B and D, p values indicate the significance of differences between the indicated data sets compared with either *cdc13-1* or *cdc23-1* controls.

et al., 1991; Shamu and Murray, 1992; Clarke *et al*., 1993; Azuma *et al*., 2005; Diaz-Martinez *et al*., 2006; Dawlaty *et al*., 2008). Second, our previous work suggested Top2 might mediate a cohesive linkage between sister *CEN*s that was potentially distinct from catenation. This is because we found that either the *top2-SNM* allele or Top2 overproduction could partially suppress a *CEN* proximal cohesion defect (Bachant *et al*., 2002). Third, Top2 has been implicated in yeast chromosome condensation (Vas *et al*., 2007). Of these functions, it was not readily apparent why increased winding or linkage between sister *CEN*s would cause kinetochores to be pulled further apart during biorientation. In contrast, a defect in maintaining *CEN* compaction seemed a reasonable hypothesis to account for the *top2 CEN* stretching phenotype. There is at present no means to assay higher order coiling within *CEN* chromatin. However, Top2 has recently been shown to be more proficient than Top1 at relaxing torsional strain on chromatin templates (Salceda *et al*., 2006), and it seemed possible that biorientation might induce alterations to superhelical winding as *CEN* fibers were placed under tension. Based on this reasoning, we decided to test whether Top2 might be required to modulate intrachromatid topology at *CEN*s.

To do this, we constructed strains in which *CEN4* was replaced with a *CEN* cassette flanked by *lox*P repeats, allowing excision of a circular *CEN* DNA molecule after Cre production under control of a galactose-inducible promoter (Figure 5A). *cdc20-1*, *cdc20-1top2-4*, and *cdc20-1top2-SNM* strains harboring *loxCENlox* were arrested in nocodazole and released into galactose media at a nonpermissive temperature for the *cdc20-1* and *top2-4* alleles. Under these conditions, spindle assembly and biorientation could proceed, but cells were prevented from going into anaphase by inactivation of the Cdc20 APC subunit. Genomic DNA was then fractionated on 2 μg/ml chloroquine gels to analyze *CEN* topoisomers. All three strains showed a similar distribution of linking number variants in the absence of tension (+NZ; Figure 5, B and C, and Supplemental Figure 4). In comparison, when kinetochores were allowed to biorient at the *cdc20* block (−NZ), we observed *CEN* loop-out products from *cdc20top2-4* cells migrating as a noticeably more relaxed set of topoisomers compared with *cdc20TOP2* controls. By analyzing these samples under a range of chloroquine concentrations, it seemed as though *CEN* circles were comparatively overwound (more positively supercoiled) in *top2-4* cells (Supplemental Figure 5). Alterations to *CEN* topology were less apparent in *cdc20top2-SNM* strains. However, by overlaying profiles of topoisomer distributions (Figure 5C and Supplemental Figure 4) it did seem that there was also a shift toward more relaxed linking number variants in *cdc20top2-SNM* samples. Thus, based on this assay, it seems that pertur-

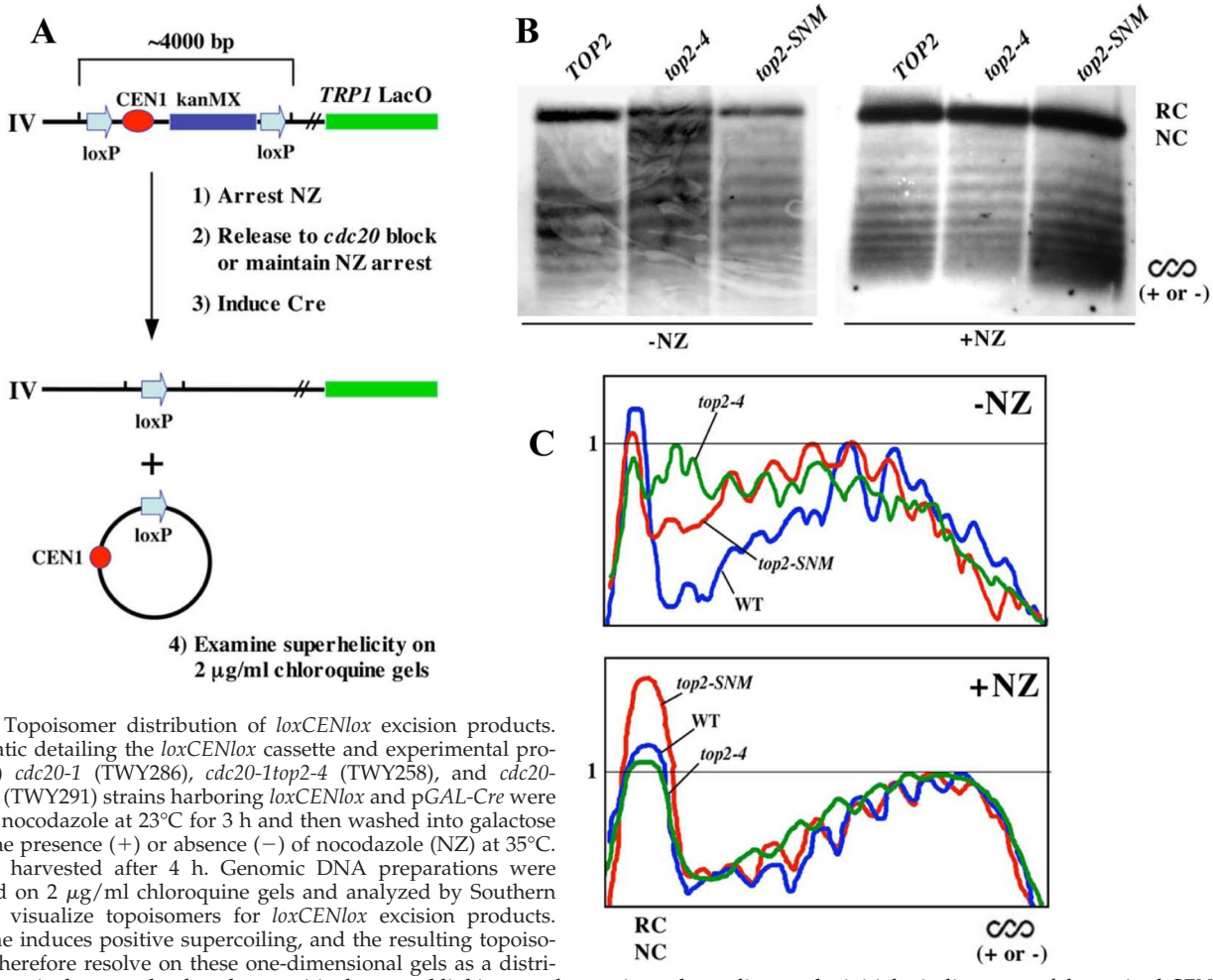

Figure 5. Topoisomer distribution of *loxCENlox* excision products. (A) Schematic detailing the *loxCENlox* cassette and experimental procedure. (B) *cdc20-1* (TWY286), *cdc20-1top2-4* (TWY258), and *cdc20-1top2-SNM* (TWY291) strains harboring *loxCENlox* and p*GAL-Cre* were arrested in nocodazole at 23°C for 3 h and then washed into galactose media in the presence (+) or absence (−) of nocodazole (NZ) at 35°C. Cells were harvested after 4 h. Genomic DNA preparations were fractionated on 2 μg/ml chloroquine gels and analyzed by Southern blotting to visualize topoisomers for *loxCENlox* excision products. Chloroquine induces positive supercoiling, and the resulting topoisomers will therefore resolve on these one-dimensional gels as a distribution of negatively wound, relaxed, or positively wound linking number variants depending on the initial winding state of the excised *CEN* circle. In all these samples, there are also likely to be nicked forms of the excision product resulting from sample preparation that will migrate as completely relaxed molecules. SC; position of either (+) or (−) supercoiled forms. RC/NC; relaxed/nicked circle. (C) To more readily compare samples, the gel panels shown in B were analyzed by densitometry to create graphical representations of topoisomer distributions. The most prominent topoisomer band was assigned a relative gray scale value of 1, and the graphs show overlays of the normalized profiles. Blue, *cdc20TOP2* (denoted on graphs as WT); green, *cdc20top2-4*; red, *cdc20top2-SNM*.

bations to Top2 are associated with alterations to *CEN* topology induced in response to tension.

Top2 Promotes Tension Checkpoint Arrest and Chromatid Detachment in Mtw1 Mutants

A particularly important question in our analysis concerned the functional significance of the role we had uncovered for Top2 in *CEN* tensioning. In particular, because chromatids bioriented and segregated properly in *top2-SNM* cells, this aspect of Top2 function did not seem to contribute markedly to chromosome stability, at least under normal conditions. As elaborated in the Introduction, however, the tensile properties of *CEN* chromatin may be one factor influencing Ipl1/Aurora B targeting of kinetochore–spindle attachment errors. Based on this idea, we considered the possibility that a function for Top2 in the ability of *CEN* chromatin to resist deformation by the spindle might become important when Ipl1 was forced to evaluate a partial reduction of bipolar tension.

Mutations affecting the kinetochore protein Mtw1 have been shown to activate Ipl1 to detach chromatids from the spindle and induce SAC arrest (Pinsky *et al*., 2003), presumably because kinetochores attach to microtubules in a weakened configuration that leads to reduced tension. Accordingly, *mtw1-1top2-4*, and *mtw1-1top2-SNM* strains, along with WT, *mtw1-1* and *mtw1-1ipl1-321* controls were released from G1 at 37°C, and SAC arrest was monitored by determining the fraction of large-budded cells and cells with nuclear Pds1 staining. *mtw1* cells arrested, whereas *mtw1ipl1* cells progressed through mitosis with similar kinetics to WT controls, indicating a complete checkpoint defect (Figure 6A). In comparison, *mtw1top2-4* and *mtw1top2-SNM* exhibited an attenuated response where SAC arrest diminished over 5 h.

If *top2-SNM* interferes with how the *mtw1* defect is perceived by Ipl1, kinetochore–spindle connections should be stabilized in *mtw1top2-SNM* strains. Indeed, the frequency of *mtw1* cells exhibiting bipolar *CEN4-GFP* attachments increased in *mtw1top2-SNM* cells at 37°C, associated with cells exhibiting stretched *CEN4-GFP* (Figure 6, C and D). Three criteria were used to address whether this restoration of attachment corresponded with improved chromosome segregation. First, the presence of the *top2-SNM* allele did not suppress *mtw1* temperature sensitivity (data not shown).

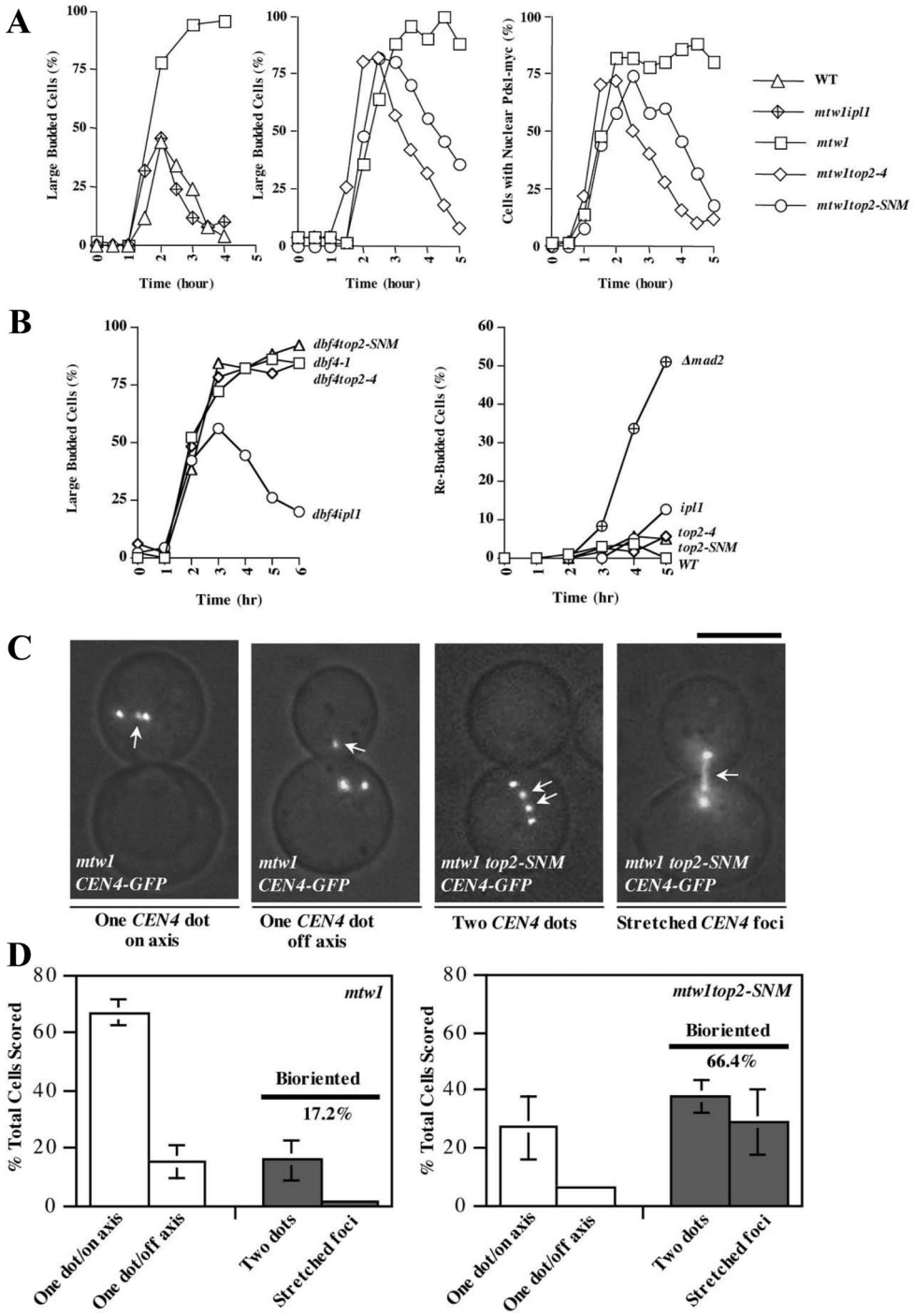

Figure 6. Tension checkpoint integrity in *top2* mutants. (A) Each graph shows a separate experiment where WT (JBY649), *mtw1-1* (JBY1544), *mtw1-1ipl1-321* (SBY1724), *mtw1-1top2-4* (JBY1560) or *mtw1-1top2-SNM* (JBY1553) *PDS1-MYC* strains were released from a G1 arrest (α-factor) at 37°C. α-factor was restored after budding to restore G1 arrest in cells that completed mitosis. The percentage of large budded cells (left and middle graphs) or cells displaying nuclear Pds1-myc immunofluorescence staining (right graph) was determined at each time point. (B) Left graph. WT (Y300), *dbf4-1* (TWY211), *dbf4-1ipl1-321* (JBY1643), *dbf4-1top2-4* (JBY1640), and *dbf4-1top2-SNM* (JBY1644) strains were released from a G1 block at 36°C and α-factor was restored after budding. The percentage of large-budded cells was determined at each time point. Right graph. WT (Y300), Δ*mad2* (JBY554), *ipl1-321* (YM311), *top2-4* (JBY335), and *top2-SNM* (JBY1452) strains were released from α-factor into nocodazole-containing media at 36°C. The percentage of rebudded cells was determined at each time point. A rebudded cell is a large budded cell that has sent out one or more additional buds, indicating a failure in SAC arrest. (C) Micrographs illustrating *CEN4-GFP* alignment categories. Arrows mark *CEN4-GFP*; unmarked foci are Spc42-GFP. Bar, 5 μm. (D) *mtw1-1 SPC42-GFP CEN4-GFP* (TW194; 3 experiments, TWY199; 1 experiment) and *mtw1-1top2-SNM SPC42-GFP CEN4-GFP* (TWY195, 196, 197, 200; 1 experiment each) strains were shifted to 37°C for 2 h before microscopy. Using Spc42-GFP to mark spindle poles, large budded cells that had not undergone spindle extension were scored into the indicated categories. Graphs depict the mean and SD for the combined experiments; in total, 506 and 514 cells were evaluated for *mtw1-1* and *mtw1top2-SNM* strains.

Second, *mtw1* cells exhibited a slight increase in chromosome loss at a semipermissive temperature of 34°C; this was not significantly reduced in *mtw1top2-SNM* strains (Supplemental Figure 6A). Third, at 35.5°C *mtw1* cells arrested only transiently, making it possible to evaluate the frequency of cells with two *TRP1-GFP* foci after completion of mitosis. A partial reduction in this segregation error was in fact observed in *mtw1top2-SNM* mutants (Supplemental Figure 6B). Overall, however, the data suggest improved kinetochore attachment in *mtw1top2-SNM* cells is not sufficient to restore chromosome segregation. This is similar to what has been documented in *mtw1ipl1* mutants; one possibility is that even though *mtw1* kinetochores are not being actively disconnected they are unable to remain attached to the spindle during anaphase (Pinsky *et al.*, 2003).

Ipl1 is also required to activate the SAC in strains defective for the initiation of DNA replication or chromatid cohesion, but not when unoccupied kinetochores are generated directly using nocodazole (Biggins and Murray, 2001). We therefore examined SAC arrest under these conditions in *top2* mutants. We observed that replication defective *top2-4dbf4-1* and *top2-SNMdbf4-1* strains arrested similarly to *dbf4-1* controls, whereas *ipl1-321dbf4-1* mutants failed to ar-

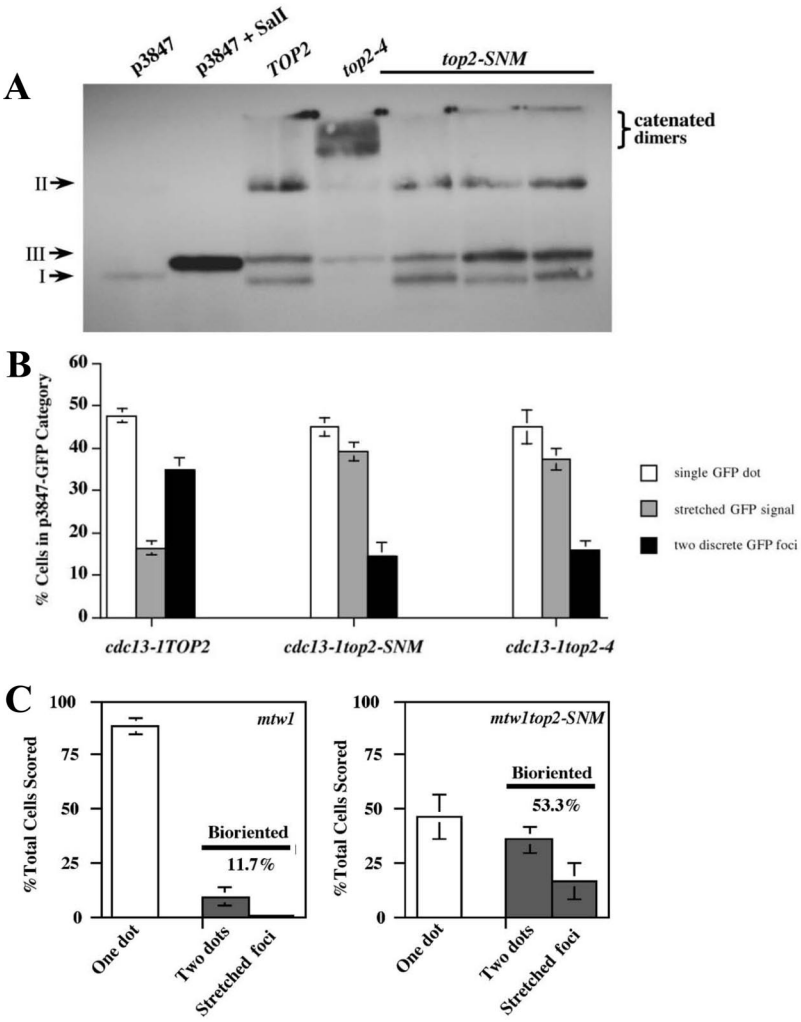

Figure 7. Analysis of minichromosome catenation, elasticity, and spindle attachment. (A) *cdc13-1* (*TOP2*; JBY1461), *cdc13-1top2-4* (JBY1462), and *cdc13-1top2-SNM* (JBY1454, 1455, 1456) strains harboring p3847 were released from α-factor at 35°C. After 3 h, p3847 electrophoretic mobility was evaluated by Southern blotting. Supercoiled (p3847) and linearized (p3847 + SalI) p3847 prepared from *E. coli* were included as controls. I, II, and III, respectively, denote supercoiled, nicked circular, and linear plasmid species. (B) *cdc13-1* (JBY1466, JBY1467; 2 experiments each), *cdc13-1top2-SNM* (JBY1473, JBY1474, JBY1471; 1 experiment each) and *cdc13-1top2-4* (JBY1476; 3 experiments) p3847 transformants were arrested at 34°C for 2.5 h before imaging. Minichromosome stretching was evaluated using the indicated categories. Graphs depict the mean and SD for the combined experiments. (C) *mtw1-1* (TWY259; 3 experiments, TWY260; 3 experiments) and *mtw1-1top2-SNM* (TWY264; three experiments, TWY265; three experiments) strains harboring p3847 were either released from α-factor or shifted as asynchronous cell culture to 37°C for 2 h before microscopy to visualize the GFP-tagged p3847 minichromosome. Large-budded cells were scored into the indicated categories. Graphs depict the mean and SD for the combined experiments; in total, 604 and 686 cells were evaluated for *mtw1-1* and *mtw1top2-SNM* strains.

rest (Figure 6B). Thus, Top2 is not required for tension checkpoint arrest if bipolar attachment is completely circumvented. In keeping with this, *top2-4* and *top2-SNM* mutants seemed largely proficient for SAC arrest after treatment with nocodazole (Figure 6B). Previous experiments have established that inactivating *top2-4* silences the tension checkpoint in strains deficient for chromatid cohesion (Dewar *et al*., 2004). To determine whether the *top2-SNM* allele behaved similarly, cohesin-deficient *scc1-73top2-4*, and *scc1-73top2-SNM* mutants were analyzed as described for *mtw1top2* strains. We observed *scc1top2-4* and *scc1top2-SNM* cells proceeded through mitosis more rapidly than *scc1* controls (Supplemental Figure 7), suggesting SAC arrest was less robust in both *top2* alleles.

Restoration of Chromatid Attachment in mtw1top2-SNM Mutants in the Absence of Catenation

In the case of *scc1top2-4* mutants, inactivation of Top2 has been proposed to silence the tension checkpoint because failure to resolve catenates provides an alternative means of linking sister chromatids and restoring tension (Dewar *et al*., 2004). Because *top2-SNM* mutants seemed to have a subtle defect in decatenating sister chromatids (Figure 1D), it was possible that checkpoint override in *scc1top2-SNM* mutants occurred through a similar mechanism. This brought into question the basis for the attenuated checkpoint response of *mtw1top2* strains; specifically, could trapped catenates restore tension to weakened *mtw1* kinetochores? To address this issue unambiguously, we examined catenation, *CEN* morphology under tension, and chromatid attachment to the spindle in *mtw1top2-SNM* cells harboring p3847, a GFP-tagged circular minichromosome containing 10.7-kb of *CEN4* flanking DNA (Tanaka *et al*., 1999). Previous studies have shown that replicated minichromosomes remain paired as sister chromatids until the metaphase to anaphase transition and are joined by cohesive linkages that are capable of supporting tension (Guacci *et al*., 1994; Megee and Koshland, 1999). Even with this relatively large minichromosome (~20 kb) catenated forms of p3847 were not observed in *cdc13* and *cdc13top2-SNM* cells, but they were readily detected in *cdc13top2-4* strains (Figure 7A; similar results were obtained in nocodazole-arrested cells; data not shown). Compared with endogenous *CEN4*, p3847 exhibited an increased tendency to adopt a filamentous configuration in *cdc13TOP2* cells during biorientation (Figures 7B and 2B). Nonetheless, the frequency of cells displaying a stretched chromatin morphology was clearly elevated in *cdc13top2-4* and *cdc13top2-SNM* transformants, again corresponding with a reduction in separated, compact GFP foci. Finally, we examined p3847 attachment to the spindle in *mtw1* and *mtw1top2-SNM* mutants (Figure 7C). After a shift to the nonpermissive temperature, the majority of *mtw1* cells

showed a single GFP dot. In contrast, *mtw1top2-SNM* strains showed a higher percentage of cells with two foci and stretched GFP-labeled chromatin, suggesting a restoration of bipolar attachment. We conclude that kinetochore–microtubule interactions can be stabilized in *mtw1top2-SNM* mutants even in the absence of catenation between sister chromatids.

DISCUSSION

In vertebrates, disruption of PIASγ or RanBP2, two SUMO ligases implicated in Topo II sumoylation, interferes with Topo II localization to *CEN*s and chromatid separation in anaphase (Azuma *et al*., 2005; Diaz-Martinez *et al*., 2006; Dawlaty *et al*., 2008). It is not known whether Top2 is targeted to yeast *CEN*s in an equivalent manner. However, Top2-SUMO fusion proteins can exhibit robust cross-linking to *CEN* DNA (Takahashi *et al*., 2006) or accumulate in the nucleolus (Takahashi and Strunnikov, 2007), indicating sumoylation may also regulate yeast Top2 trafficking. In this report, we used the *top2-SNM* allele to specifically examine functions associated with Top2 SUMO modification, comparing *top2-SNM* strains to catalytically inactive *top2-4* mutants. The two main phenotypes we observed were a tendency for *CEN*s to adopt a drawn out, filamentous appearance as kinetochores bioriented on the spindle and a defect in sustaining tension checkpoint arrest in kinetochore- and cohesin-defective strains. As discussed below, these observations suggest a novel role for Top2 in maintaining tensile *CEN*s that seems to be connected to enforcing aspects of the tension checkpoint.

Top2 Function in CEN Tensioning

Based on increased *CEN* stretching, interkinetochore distance, and preanaphase spindle extension, a main conclusion from this study is that Top2 acts in some capacity to allow *CEN*s to resist the force of the spindle. There are two aspects to this. First, because increased stretching occurs in both *top2-SNM* and *top2-4* mutants the simplest interpretation is that sumoylation promotes Top2 function in limiting *CEN* expansion, although we cannot exclude that different defects are responsible for *CEN* stretching in *top2-4* and *top2-SNM* strains. Second, this aspect of Top2 function seems to be separable from decatenation, which has been considered the main *CEN* function for TopoII. Most directly, as evaluated using a topologically closed minichromosome, increased stretching occurred in *top2-SNM* cells even in the absence of catenation.

One hypothesis to explain our data are that Top2 modulates *CEN* tensioning by reinforcing a compact *CEN* structure. This might be in keeping with the observation that treating vertebrate cells with the TopoII inhibitor ICRF-193 disorganizes *CEN* chromatin (Rattner *et al*., 1996). At present, we can only speculate as to how Top2 might mediate *CEN* compaction. Because Top2 binds DNA as a dimer, Top2 could act in a structural role to stabilize DNA loops (Aguilar *et al*., 2005), potentially facilitating coiling within the paired *CEN* foci that form during biorientation.

Top2 could also maintain *CEN* compaction in its capacity as a topoisomerase. Our *CEN* excision experiments are consistent with this, because they reveal *top2* mutants display altered *CEN* superhelicity when chromatids are placed under tension. This may suggest Top2 is required to relax topological stress induced during biorientation, although it is also possible that perturbations to Top2 are a direct cause of aberrant changes to *CEN* topology. We can envision at least two ways in which torsional strain might arise as *CEN*s are placed under tension. In vitro pulling experiments have shown that DNA overwinds when stretched (Gore *et al*., 2006), and it is therefore possible that tension could sufficiently distort the DNA helix to alter topology. Alternatively, *CEN* chromatin unravels extensively during biorientation, potentially to a point where nucleosomes are displaced as a means to dissipate tension (He *et al*., 2000; Pearson *et al*., 2001). This would be expected to release superhelical turns constrained by the nucleosomes. Interestingly, a recent study has shown there is in fact a relationship between nucleosome packaging and *CEN* elasticity, with reduced nucleosome density producing exacerbated *CEN* stretching and spindle extension (Bouck and Bloom, 2007), reminiscent of *top2* mutants.

Finally, a role for Top2 in *CEN* compaction could be mediated through a functional interaction with the condensin complex. Condensin can reconfigure DNA topology in a Topo II-dependent manner (Stray *et al*., 2005) and has been suggested to localize to yeast *CEN*s (Bachellier-Bassi *et al*., 2008). Condensin has also been implicated in preventing *CEN* expansion under tension (Oliveira *et al*., 2005; Gerlich *et al*., 2006; Yong-Gonzalez *et al*., 2007).

Top2 Function in the Tension Checkpoint

Topo II inactivation silences the SAC and stabilizes chromatid-spindle attachment in cohesin-deficient cells, probably reflecting the ability of unresolved catenates to restore tension (Dewar *et al*., 2004; Vagnarelli *et al*., 2004; Toyoda and Yanagida, 2006). In our experiments, restoration of chromatid-spindle attachments in *mtw1top2-SNM* mutants did not require catenation between sister *CEN*s and was not accompanied by suppression of the underlying *mtw1* kinetochore defect. Thus, if *top2-SNM* causes an increase in interkinetochore tension that compensates for *mtw1* kinetochores, this presumably occurs through an as yet unknown mechanism. Such an increase in tension would also be counterintuitive to kinetochores being pulled further apart in *top2-SNM* strains. One scenario, however, is that perturbations to kinetochore structure or geometry in *top2-SNM* or *top2-4* mutants (potentially associated with alterations to *CEN* chromatin structure) could make it more difficult for Ipl1 to phosphorylate kinetochore substrates or could allow kinetochore reattachment to occur more efficiently.

A distinct view, prompted by tensiometer models invoking *CEN* stretching as a factor controlling Ipl1/Aurora B targeting of kinetochores, is that in *mtw1top2* mutants weakened kinetochores can distend *CEN*s into a configuration that mimics tension. The observation that Top2 is not required for Ipl1 to respond to monopolar attachments in replication-defective *dbf4-1* mutants is consistent with this; in the absence of bipolar force it presumably becomes unnecessary to calibrate *CEN* resistance to spindle pulling. By extension, Top2 would not be expected to play a role in resolving syntelic attachments, explaining the normal chromosome loss rate of *top2-SNM* strains. Further analysis of Ipl1 localization and activity in *top2* mutants may help shed light on whether there actually is a mechanistic coupling between *CEN* stretching and stabilization of *mtw1* kinetochore attachments.

A model in which Top2 enforces the sensitivity of the tension checkpoint would seem to contrast with reports indicating perturbations to Topo II activate metaphase arrest through pathways that overlap extensively, if are not identical to, the SAC (Mikhailov *et al*., 2002; Skoufias *et al*., 2004; Clarke *et al*., 2006; Diaz-Martinez *et al*., 2006; Toyoda and Yanagida, 2006). The signal(s) that elicits this arrest has been controversial, with one suggestion being unresolved cate-

nates activate a Topo II-responsive checkpoint (Skoufias *et al*., 2004; Clarke *et al*., 2006). Although this has remained unclear, metaphase delay after Topo II inhibition has recently been shown to be abolished by the Aurora B inhibitor ZM447439 (Diaz-Martinez *et al*., 2006). Similarly, in budding yeast a new group of *top2* alleles has been identified that delay anaphase in an Ipl1-dependent manner (Andrews *et al*., 2006). If Topo II influences both *CEN* decatenation and compaction, perturbations to Topo II could have variable outcomes with respect to Ipl1/Aurora B signaling. For example, depleting Topo II in vertebrate cells where sister *CEN*s seems to be tightly linked by catenation has been reported to lead to a shortened metaphase interkinetochore distance (Spence *et al*., 2007), which could possibly simulate a reduction in tension. In contrast, if sister *CEN*s were not extensively joined by catenates, or if it were possible to specifically perturb Topo II *CEN* compaction activity, *CEN* fibers might distend more easily into a configuration that conferred resistance to the tension checkpoint. Such a framework may prove useful for analyzing what is turning out to be a complex set of interactions between Topo II, *CEN* mechanics, and the tension branch of the SAC.

ACKNOWLEDGMENTS

We thank Drs. S. Biggins, S. Elledge, P. Hieter, A. Murray, and K. Nasmyth for generously providing strains and reagents. We also thank Drs. S. Biggins, K. Bloom, D. Clarke, C. Nugent, and members of the Bachant laboratory for useful comments on the manuscript and insightful discussions. This work was supported by National Institutes of Health grant GM-66190 (to J. B.).

REFERENCES

Aguilar, C., Davidson, C., Dix, M., Stead, K., Zheng, K., Hartman, T., and Guacci, V. (2005). Topoisomerase II suppresses the temperature sensitivity of *Saccharomyces cerevisiae pds5* mutants, but not the defect in sister chromatid cohesion. Cell Cycle *4*, 1294–1304.

Andrews, C. A., Vas, A. C., Meier, B., Gimenez-Abian, J. F., Diaz-Martinez, L. A., Green, J., Erickson, S. L., Vanderwaal, K. E., Hsu, W. S., and Clarke, D. J. (2006). A mitotic topoisomerase II checkpoint in budding yeast is required for genome stability but acts independently of Pds1/securin. Genes Dev. *20*, 1162–1174.

Azuma, Y., Arnaoutov, A., Anan, T., and Dasso, M. (2005). PIASy mediates SUMO-2 conjugation of Topoisomerase-II on mitotic chromosomes. EMBO J. *24*, 2172–2182.

Azuma, Y., Arnaoutov, A., and Dasso, M. (2003). SUMO-2/3 regulates topoisomerase II in mitosis. J. Cell Biol. *163*, 477–487.

Bachant, J., Alcasabas, A., Blat, Y., Kleckner, N., and Elledge, S. J. (2002). The SUMO-1 isopeptidase Smt4 is linked to centromeric cohesion through SUMO-1 modification of DNA topoisomerase II. Mol. Cell *9*, 1169–1182.

Bachant, J., Jessen, S. R., Kavanaugh, S. E., and Fielding, C. S. (2005). The yeast S phase checkpoint enables replicating chromosomes to bi-orient and restrain spindle extension during S phase distress. J. Cell Biol. *168*, 999–1012.

Bachellier-Bassi, S., Gadal, O., Bourout, G., and Nehrbass, U. (2008). Cell cycle-dependent kinetochore localization of condensin complex in *Saccharomyces cerevisiae*. J. Struct. Biol. *162*, 248–259.

Bhalla, N., Biggins, S., and Murray, A. W. (2002). Mutation of *YCS4*, a budding yeast condensin subunit, affects mitotic and nonmitotic chromosome behavior. Mol. Biol. Cell *13*, 632–645.

Biggins, S., and Murray, A. W. (2001). The budding yeast protein kinase Ipl1/Aurora allows the absence of tension to activate the spindle checkpoint. Genes Dev. *15*, 3118–3129.

Bouck, D. C., and Bloom, K. (2007). Pericentric chromatin is an elastic component of the mitotic spindle. Curr. Biol. *17*, 741–748.

Cimini, D. (2007). Detection and correction of merotelic kinetochore orientationby Aurora B and its partners. Cell Cycle *6*, 1558–1564.

Clarke, D. J., Johnson, R. T., and Downes, C. S. (1993). Topoisomerase II inhibition prevents anaphase chromatid segregation in mammalian cells independently of the generation of DNA strand breaks. J. Cell Sci. *105*, 563–569.

Clarke, D. J., Vas, A. C., Andrews, C. A., Diaz-Martinez, L. A., and Gimenez-Abian, J. F. (2006). Topoisomerase II checkpoints: universal mechanisms that regulate mitosis. Cell Cycle *5*, 1925–1928.

Dawlaty, M. M., Malureanu, L., Jeganathan, K. B., Kao, E., Sustmann, C., Tahk, S., Shuai, K., Grosschedl, R., and van Deursen, J. M. (2008). Resolution of sister centromeres requires RanBP2-mediated SUMOylation of topoisomerase IIalpha. Cell *133*, 103–115.

Dewar, H., Tanaka, K., Nasmyth, K., and Tanaka, T. U. (2004). Tension between two kinetochores suffices for their bi-orientation on the mitotic spindle. Nature *428*, 93–97.

Diaz-Martinez, L. A., Gimenez-Abian, J. F., Azuma, Y., Guacci, V., Gimenez-Martin, G., Lanier, L. M., and Clarke, D. J. (2006). PIASgamma is required for faithful chromosome segregation in human cells. PLoS ONE *1*, e53.

DiNardo, S., Voelkel, K., and Sternglanz, R. (1984). DNA topoisomerase II mutant of *Saccharomyces cerevisiae*: topoisomerase II is required for segregation of daughter molecules at the termination of DNA replication. Proc. Natl. Acad. Sci. USA *81*, 2616–2620.

Downes, C. S., Mullinger, A. M., and Johnson, R. T. (1991). Inhibitors of DNA topoisomerase II prevent chromatid separation in mammalian cells but do not prevent exit from mitosis. Proc. Natl. Acad. Sci. USA *88*, 8895–8899.

Eckert, C. A., Gravdahl, D. J., and Megee, P. C. (2007). The enhancement of pericentromeric cohesin association by conserved kinetochore components promotes high-fidelity chromosome segregation and is sensitive to microtubule-based tension. Genes Dev. *21*, 278–291.

Garvik, B., Carson, M., and Hartwell, L. (1995). Single-stranded DNA arising at telomeres in *cdc13* mutants may constitute a specific signal for the *RAD9* checkpoint. Mol. Cell. Biol. *15*, 6128–6138.

Gerlich, D., Hirota, T., Koch, B., Peters, J. M., and Ellenberg, J. (2006). Condensin I stabilizes chromosomes mechanically through a dynamic interaction in live cells. Curr. Biol. *16*, 333–344.

Gore, J., Bryant, Z., Nollmann, M., Le, M. U., Cozzarelli, N. R., and Bustamante, C. (2006). DNA overwinds when stretched. Nature *442*, 836–839.

Goshima, G., and Yanagida, M. (2000). Establishing biorientation occurs with precocious separation of the sister kinetochores, but not the arms, in the early spindle of budding yeast. Cell *100*, 619–633.

Guacci, V., Hogan, E., and Koshland, D. (1994). Chromosome condensation and sister chromatid pairing in budding yeast. J. Cell Biol. *125*, 517–530.

He, X., Asthana, S., and Sorger, P. K. (2000). Transient sister chromatid separation and elastic deformation of chromosomes during mitosis in budding yeast. Cell *101*, 763–775.

Hieter, P., Mann, C., Snyder, M., and Davis, R. W. (1985). Mitotic stability of yeast chromosomes: a colony color assay that measures nondisjunction and chromosome loss. Cell *40*, 381–392.

Holm, C. (1994). Coming undone: how to untangle a chromosome. Cell *77*, 955–957.

Holm, C., Goto, T., Wang, J. C., and Botstein, D. (1985). DNA topoisomerase II is required at the time of mitosis in yeast. Cell *41*, 553–563.

Holm, C., Stearns, T., and Botstein, D. (1989). DNA topoisomerase II must act at mitosis to prevent nondisjunction and chromosome breakage. Mol. Cell. Biol. *9*, 159–168.

King, E. M., Rachidi, N., Morrice, N., Hardwick, K. G., and Stark, M. J. (2007). Ipl1p-dependent phosphorylation of Mad3p is required for the spindle checkpoint response to lack of tension at kinetochores. Genes Dev. *21*, 1163–1168.

Koshland, D., and Hartwell, L. H. (1987). The structure of sister minichromosome DNA before anaphase in *Saccharomyces cerevisiae*. Science *238*, 1713–1716.

Li, Y., Bachant, J., Alcasabas, A. A., Wang, Y., Qin, J., and Elledge, S. J. (2002). The mitotic spindle is required for loading of the DASH complex onto the kinetochore. Genes Dev. *16*, 183–197.

McIntosh, J. R. (1991). Structural and mechanical control of mitotic progression. Cold Spring Harb. Symp. Quant. Biol. *56*, 613–619.

Megee, P. C., and Koshland, D. (1999). A functional assay for centromere-associated sister chromatid cohesion. Science *285*, 254–257.

Mikhailov, A., Cole, R. W., and Rieder, C. L. (2002). DNA damage during mitosis in human cells delays the metaphase/anaphase transition via the spindle-assembly checkpoint. Curr. Biol. *12*, 1797–1806.

Murakami, S., Yanagida, M., and Niwa, O. (1995). A large circular minichromosome of *Schizosaccharomyces pombe* requires a high dose of type II DNA topoisomerase for its stabilization. Mol. Gen. Genet. *246*, 671–679.

Ocampo-Hafalla, M. T., Katou, Y., Shirahige, K., and Uhlmann, F. (2007). Displacement and re-accumulation of centromeric cohesin during transient pre-anaphase centromere splitting. Chromosoma *116*, 531–544.

Oliveira, R. A., Coelho, P. A., and Sunkel, C. E. (2005). The condensin I subunit Barren/CAP-H is essential for the structural integrity of centromeric heterochromatin during mitosis. Mol. Cell. Biol. *25*, 8971–8984.

Pearson, C. G., Maddox, P. S., Salmon, E. D., and Bloom, K. (2001). Budding yeast chromosome structure and dynamics during mitosis. J. Cell Biol. *152*, 1255–1266.

Pinsky, B. A., and Biggins, S. (2005). The spindle checkpoint: tension versus attachment. Trends Cell Biol. *15*, 486–493.

Pinsky, B. A., Kung, C., Shokat, K. M., and Biggins, S. (2006). The Ipl1-Aurora protein kinase activates the spindle checkpoint by creating unattached kinetochores. Nat. Cell Biol. *8*, 78–83.

Pinsky, B. A., Tatsutani, S. Y., Collins, K. A., and Biggins, S. (2003). An Mtw1 complex promotes kinetochore biorientation that is monitored by the Ipl1/Aurora protein kinase. Dev. Cell *5*, 735–745.

Porter, A. C., and Farr, C. J. (2004). Topoisomerase II: untangling its contribution at the centromere. Chromosome Res. *12*, 569–583.

Rattner, J. B., Hendzel, M. J., Furbee, C. S., Muller, M. T., and Bazett-Jones, D. P. (1996). Topoisomerase II alpha is associated with the mammalian centromere in a cell cycle- and species-specific manner and is required for proper centromere/kinetochore structure. J. Cell Biol. *134*, 1097–1107.

Ruchaud, S., Carmena, M., and Earnshaw, W. C. (2007). Chromosomal passengers: conducting cell division. Nat. Rev. Mol. Cell Biol. *8*, 798–812.

Salceda, J., Fernandez, X., and Roca, J. (2006). Topoisomerase II, not topoisomerase I, is the proficient relaxase of nucleosomal DNA. EMBO J. *25*, 2575–2583.

Sandall, S., Severin, F., McLeod, I. X., Yates, J. R., 3rd, Oegema, K., Hyman, A., and Desai, A. (2006). A Bir1-Sli15 complex connects centromeres to microtubules and is required to sense kinetochore tension. Cell *127*, 1179–1191.

Sauer, B. (1987). Functional expression of the *cre-lox* site-specific recombination system in the yeast *Saccharomyces cerevisiae*. Mol. Cell. Biol. *7*, 2087–2096.

Shamu, C. E., and Murray, A. W. (1992). Sister chromatid separation in frog egg extracts requires DNA topoisomerase II activity during anaphase. J. Cell Biol. *117*, 921–934.

Shelby, R. D., Hahn, K. M., and Sullivan, K. F. (1996). Dynamic elastic behavior of alpha-satellite DNA domains visualized in situ in living human cells. J. Cell Biol. *135*, 545–557.

Skoufias, D. A., Lacroix, F. B., Andreassen, P. R., Wilson, L., and Margolis, R. L. (2004). Inhibition of DNA decatenation, but not DNA damage, arrests cells at metaphase. Mol. Cell *15*, 977–990.

Spell, R. M., and Holm, C. (1994). Nature and distribution of chromosomal intertwinings in *Saccharomyces cerevisiae*. Mol. Cell. Biol. *14*, 1465–1476.

Spence, J. M., Phua, H. H., Mills, W., Carpenter, A. J., Porter, A. C., and Farr, C. J. (2007). Depletion of topoisomerase IIalpha leads to shortening of the metaphase interkinetochore distance and abnormal persistence of PICH-coated anaphase threads. J. Cell Sci. *120*, 3952–3964.

Spencer, F., Gerring, S. L., Connelly, C., and Hieter, P. (1990). Mitotic chromosome transmission fidelity mutants in *Saccharomyces cerevisiae*. Genetics *124*, 237–249.

Stray, J. E., Crisona, N. J., Belotserkovskii, B. P., Lindsley, J. E., and Cozzarelli, N. R. (2005). The *Saccharomyces cerevisiae* Smc2/4 condensin compacts DNA into (+) chiral structures without net supercoiling. J. Biol. Chem. *280*, 34723–34734.

Takahashi, Y., and Strunnikov, A. (2007). In vivo modeling of polysumoylation uncovers targeting of Topoisomerase II to the nucleolus via optimal level of SUMO modification. Chromosoma *117*, 189–198.

Takahashi, Y., Yong-Gonzalez, V., Kikuchi, Y., and Strunnikov, A. (2006). SIZ1/SIZ2 control of chromosome transmission fidelity is mediated by the sumoylation of topoisomerase II. Genetics *172*, 783–794.

Tanaka, T., Cosma, M. P., Wirth, K., and Nasmyth, K. (1999). Identification of cohesin association sites at centromeres and along chromosome arms. Cell *98*, 847–858.

Tanaka, T., Fuchs, J., Loidl, J., and Nasmyth, K. (2000). Cohesin ensures bipolar attachment of microtubules to sister centromeres and resists their precocious separation. Nat. Cell Biol. *2*, 492–499.

Tanaka, T. U., Rachidi, N., Janke, C., Pereira, G., Galova, M., Schiebel, E., Stark, M. J., and Nasmyth, K. (2002). Evidence that the Ipl1-Sli15 (Aurora kinase-INCENP) complex promotes chromosome bi-orientation by altering kinetochore-spindle pole connections. Cell *108*, 317–329.

Toyoda, Y., and Yanagida, M. (2006). Coordinated requirements of human topo II and cohesin for metaphase centromere alignment under Mad2-dependent spindle checkpoint surveillance. Mol. Biol. Cell *17*, 2287–2302.

Vagnarelli, P., Morrison, C., Dodson, H., Sonoda, E., Takeda, S., and Earnshaw, W. C. (2004). Analysis of Scc1-deficient cells defines a key metaphase role of vertebrate cohesin in linking sister kinetochores. EMBO Rep. *5*, 167–171.

Vas, A. C., Andrews, C. A., Kirkland Matesky, K., and Clarke, D. J. (2007). In vivo analysis of chromosome condensation in *Saccharomyces cerevisiae*. Mol. Biol. Cell *18*, 557–568.

Wach, A., Brachat, A., Pohlmann, R., and Philippsen, P. (1994). New heterologous modules for classical or PCR-based gene disruptions in. *Saccharomyces cerevisiae*. Yeast *10*, 1793–1808.

Yeh, E., Haase, J., Paliulis, L. V., Joglekar, A., Bond, L., Bouck, D., Salmon, E. D., and Bloom, K. S. (2008). Pericentric chromatin is organized into an intramolecular loop in mitosis. Curr. Biol. *18*, 81–90.

Yong-Gonzalez, V., Wang, B. D., Butylin, P., Ouspenski, I., and Strunnikov, A. (2007). Condensin function at centromere chromatin facilitates proper kinetochore tension and ensures correct mitotic segregation of sister chromatids. Genes Cells *12*, 1075–1090.